Design, Synthesis and Evaluation of Novel Coumarin-Carbamate Hybrids as Acetylcholinesterase Inhibitors for Alzheimer's Disease

Pun Chirat, Thongchai Kanchanasuwan, Wetchaporn Wetchakit, Sutthatip Markmee, and Ruengwit Kitbunnadaj*

Department of Pharmaceutical Chemistry and Pharmacognosy, Faculty of Pharmaceutical Sciences, Naresuan University, Phitsanulok, 65000, Thailand

* Corresponding author. E-mail address: ruengwitk@nu.ac.th

Received: 5 June 2025; Revised: 20 August 2025; Accepted: 8 September 2025; Available online: 11 September 2025

Abstract

Alzheimer's disease (AD) is the most prevalent form of dementia in elderly populations and is associated with the reduction of acetylcholine (ACh) neurotransmitter levels due to neuronal degeneration and acetylcholinesterase (AChE)-catalyzed hydrolysis. Thus, AChE inhibition represents a primary therapeutic target for AD treatment. Current first-line therapies for mild to moderate AD include acetylcholinesterase inhibitors (AChEIs) such as galantamine, donepezil, and rivastigmine. Donepezil inhibits AChE activity through interactions with the peripheral anionic site (PAS), thereby impeding amyloid-beta aggregation. Conversely, rivastigmine acts as a pseudo-irreversible inhibitor through carbamylation of the serine residue at the catalytic site (CS). In this study, we designed a novel series of compounds capable of pseudo-irreversibly inhibiting AChE while simultaneously interacting with the PAS. The coumarin nucleus was selected as the core structure for PAS interaction, with an additional carbamate group incorporated as the key functionality for carbamylation reactions at the CS. Specifically, 7-hydroxycoumarin was linked to a phenyl carbamate moiety using spacers of varying methylene units (2-7). Preliminary evaluations revealed that compound RKNU153 exhibited promising AChE inhibitory activity with 63.7% inhibition, and RKNU154 exhibited AChE inhibitory activity with 73.8% inhibition, at 100 μM concentration. However, carbamylation on the serine residue at the catalytic site of our compounds was not successful, being unable to engage in this critical interaction.

Keywords: Alzheimer's disease, Acetylcholinesterase inhibitors, Coumarin, Carbamate

Introduction

Alzheimer's disease (AD) represents a progressive neurodegenerative disorder and constitutes the predominant cause of dementia in individuals aged 65 and above. The disease manifests primarily through cognitive impairments, particularly learning and memory functions. In the United States specifically, the number of people aged 65 and older with Alzheimer's dementia is projected to increase dramatically to 13.8 million by 2050, from 4.7 million in 2010, with the largest growth in the 85+ age group, expected to reach 7.0 million. The burden of disease in most countries has been showing an increasing trend. (Chaudhary et al., 2024; Chen et al., 2025; Hebert et al., 2013; Lanctôt et al., 2024; Liu et al., 2025)

The pathophysiology of AD involves complex interactions across multiple neurotransmitter systems. Three principal hallmarks are considered central to AD pathogenesis: β-amyloid (Aβ) plaques, neurofibrillary tangles, and neuronal cell death. Aβ plaques consist of insoluble peptides resulting from aberrant cleavage of amyloid precursor protein (APP) through sequential processing by β-secretase and γ-secretase. These insoluble Aβ peptides aggregate into characteristic plaques that contribute significantly to neurotransmitter deficits and neuronal death. Most notably, AD is characterized by substantial cholinergic neuron loss and consequent reduction in

acetylcholine (ACh) levels, a neurotransmitter critical for cognitive function. Indeed, cholinergic abnormalities represent the most significant neurotransmitter alterations observed in AD (Morrison & Lyketsos, 2005).

Acetylcholine is primarily hydrolyzed by acetylcholinesterase (AChE) and butyrylcholinesterase (BuChE). AChE, in particular, plays a key role in the progression of AD and various neuronal deterioration processes (Bennion et al., 2013; Gupta et al., 2011). Consequently, acetylcholinesterase inhibitors (AChEIs) have been investigated as therapeutic agents to elevate ACh levels in the brain. Current clinical AChEIs are employed for symptomatic management of mild to moderate AD (Dvir et al., 2010; Yiannopoulou & Papageorgiou, 2020). Beyond increasing synaptic ACh concentration, these compounds demonstrate additional benefits, including protection against free radical toxicity and Aβ-induced damage, while enhancing antioxidant production (Bartus et al., 1982; Garcia-Ayllon et al., 2011).

Current AChEIs are classified into two categories (Cohen et al., 1991) based on their mechanism of action: reversible and pseudo-irreversible inhibitors (Fig. 1). Reversible AChEIs such as galantamine and donepezil competitively bind to AChE through non-covalent interactions (π-π stacking and cation-π interactions). X-ray crystallographic analysis reveals that donepezil interacts with Trp279 at the peripheral anionic site (PAS), Trp84 at the mid-gorge site (MGS), and His440 at the catalytic site (CS) (Kryger et al., 1999). In contrast, pseudo-irreversible AChEIs like rivastigmine form covalent bonds with the enzyme through carbamylation reactions, specifically targeting a serine residue at the CS and resulting in significantly slower enzyme reactivation rates than reversible inhibitors (Bar-On et al., 2002; Bartolini et al., 2007; Chaudhaery et al., 2010; Singh et al., 2023). The X-ray crystal structures of donepezil and rivastigmine with Torpedo acetylcholinesterase (*Tc*AChE) are shown in Fig. 2.

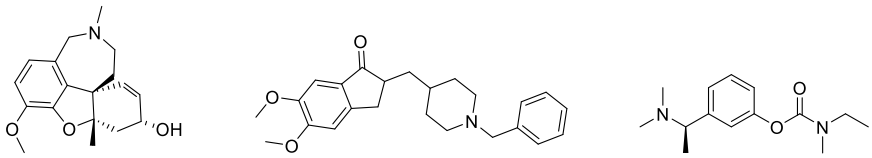

Figure 1 Chemical structures of reversible acetylcholinesterase inhibitors (galantamine and donepezil) and pseudo-irreversible acetylcholinesterase inhibitors (rivastigmine)

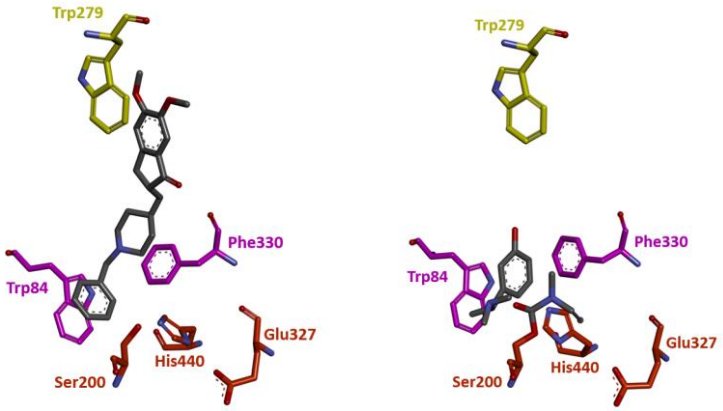

Figure 2 X-ray crystal structures of donepezil/*Tc*AChE (left) and rivastigmine/*Tc*AChE (right) obtained from PCSB Protein Data Bank: 1EVE and 1GQR, respectively. For clarity, some amino acids are omitted

Recent advances in AChE inhibitor design have focused on developing dual-binding inhibitors capable of simultaneously targeting both the active site and the PAS (de Souza et al., 2019; De Vita et al., 2016; Singh et al., 2023; Song et al., 2021; Zueva et al., 2019). The significance of this approach lies in the established interaction between Aβ peptides and AChE through a hydrophobic region proximal to the enzyme's PAS, which promotes Aβ fibril formation (Carvajal & Inestrosa, 2011; De Ferrari et al., 2001; Inestrosa et al., 2005). Molecular dynamics simulations have identified that the *Tc*AChE motif promoting Aβ fibril formation contains the conserved Trp279 (corresponding to Trp286 in human AChE), which constitutes a component of the PAS (Inestrosa et al., 2008). Thus, compounds that interact with the PAS may provide the additional benefit of inhibiting Aβ aggregation beyond their cholinesterase inhibitory activity.

Our laboratory recently identified a novel coumarin derivative (RKNU026) (see Fig. 3) as a potent AChE inhibitor with an IC_{50} value of 0.3 μM (Hiranyaekaphap et al., 2014). This compound engages in non-covalent π-π interactions with Trp279 at the PAS while its piperidine nitrogen interacts with Phe330 at the MGS through cation-π interactions, functioning as a reversible AChE inhibitor with additional Aβ-aggregation inhibitory properties (Amin et al., 2021; Bar-On et al., 2002; Lomlim & Nualnoi, 2011; Singbut & Kaewket, 2010; Sun et al., 2014). Despite these advances, a significant gap remains in the development of compounds that combine pseudo-irreversible inhibition at the catalytic site with interaction at the PAS to potentially address both cholinergic deficits and amyloid pathology simultaneously.

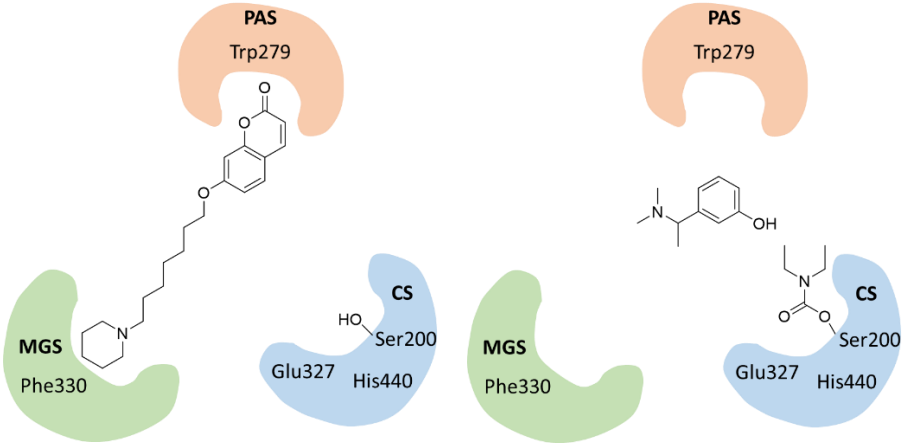

Figure 3 2D diagram represents X-ray crystal structure of RKNU026/*Tc*AChE (left) and rivastigmine/*Tc*AChE (right) obtained from PDB:1GQR. For clarity, some amino acids are omitted

In the present study, we designed a series of novel carbamate analogues incorporating a coumarin nucleus, using RKNU026 as a structural template. The design features a coumarin moiety linked to a carbamate functionality via spacers of varying lengths, ranging from two to seven methylene units. We integrated the carbamate group with the expectation that, similar to established carbamate AChEIs such as rivastigmine (Fig. 3), these compounds would covalently bind to AChE in a pseudo-irreversible manner through carbamylation of the serine residue at the catalytic site (CS). Simultaneously, we anticipated that the coumarin portion would engage with the tryptophan residue at the peripheral anionic site (PAS), thereby potentially disrupting the Aβ-aggregation process (Fig. 4).

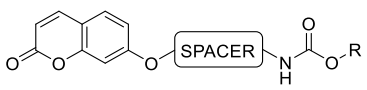

R = phenyl group and/or 7-hydroxycoumarin derivatives

SPACER = various methylene units

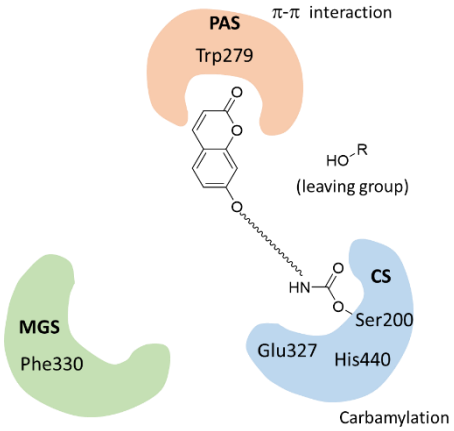

Figure 4 Proposed interaction model of novel coumarin-containing carbamate analogues with AChE: the coumarin moiety engages with the peripheral anionic site (PAS), while the basic amine forms interactions with the mid-gorge site (MGS)

Materials and Methods

Materials

All reagents were purchased from commercial suppliers and were used without further purification. Solvents used were either commercial or AR grade. All microwave (MW)-assisted reactions were carried out with Biotage Initiator Classic. Thin-layer chromatography (TLC) was performed using silica gel plates (Merck Kieselgel 60 F254), and column chromatography was performed using Biotage Isolera One flash column chromatography with silica gel SNAP cartridge (porosity 44 Å, particle size 30-90 μm, surface area 500-600 m^2/g). Melting points were determined on a Buchi B-535 melting point apparatus and are uncorrected. ^1H NMR spectra were recorded on a Bruker Advance 400 spectrometer at 400 MHz using the residual undeuterated solvent peak as reference. High-Resolution Mass Spectra (HRMS) were obtained on an Agilent 6540 UHD Accurate-Mass Q-TOF mass LC/MS spectrometer using electrospray ionization (ESI).

Methods

Compounds 1-4 were synthesized as illustrated in Figure 5. The commercially available 7-hydroxy coumarin, 7-hydroxy-2H-chromen-2-one, was alkylated with corresponding dibromoalkanes in the presence of potassium carbonate to give 7-bromoalkyloxy-2H-chromen-2-one **(1a-f)**. Next, the compound **1a-1f** was treated with sodium azide in water to give the 7-(azidoalkyloxy)-2H-chromen-2-one **(2a-2f)**. Then, the compound 2a-f was treated with ammonium chloride in 25% water in ethanol with the presence of zinc to give the 7-(aminoalkoxy)-2H-chromen-2-one **(3a-3f)**. Finally, the compounds **3a-3f** were reacted with phenyl chloroformate in dichloromethane (DCM) with the presence of triethylamine (TEA) to give the desired carbamate derivatives **4a-4f**.

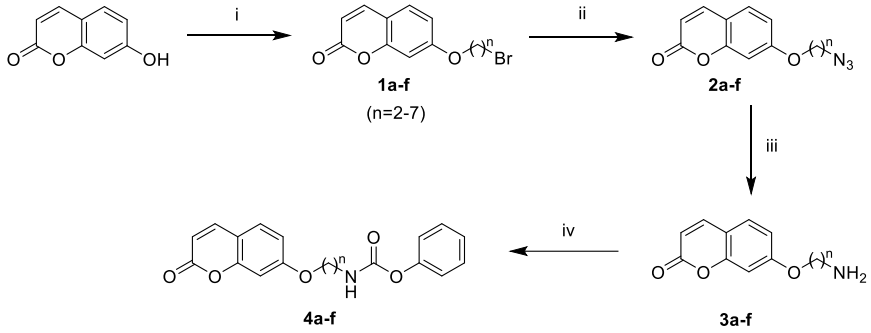

Figure 5 Synthetic pathway for compound **4a-4f**

Reagent and condition: (i) $Br-(CH_2)_n-Br$, acetone, K_2CO_3, MW 140°C 1 hr. (ii) NaN_3, water, MW 150°C 1 hr. (iii) NH_4Cl, Zn, ethanol/water (3:1), MW 150°C 1 hr. (iv) Phenyl Chloroformate, Triethylamine, Dichloromethane, 0°C for 30 min.

General procedures for synthesis of 7-bromoalkyloxy-2H-chromen-2-one derivatives (1a-1f)

7-Hydroxycoumarin (1 g, 6.16 mmol), powder of potassium carbonate (12.32 mmol), and corresponding dibromoalkane (30.80 mmol) were added to acetone (20 mL), and the mixture was irradiated at 140°C for 60 min using a microreactor. The solvent was removed under reduced pressure, 40 mL DCM was added, and the mixture was washed with sodium carbonate solution (3 x 40 mL). The organic layer was dried over sodium sulfate, and the solvent was removed under reduced pressure. The desired product was obtained after purification using flash column chromatography (DCM).

7-(2-bromoethoxy)-2H-chromen-2-one (1a). A white solid (yield 85%). ^{1}H NMR (400 MHz, $CDCl_3$) δ: 3.67 (t, 2H, *J* = 6.09 Hz), 4.35 (t, 2H, *J* = 6.10 Hz), 6.27 (d, 1H, *J* = 9.49 Hz), 6.81 (d, 1H, *J* = 2.37 Hz), 6.87 (dd, 1H, *J* = 2.47 and 8.59 Hz), 7.38 (d, 1H, *J* = 8.60 Hz), 7.64 (d, 1H, *J* = 9.49 Hz).

7-(3-bromopropoxy)-2H-chromen-2-one (1b). A white solid (yield 88%). ^{1}H NMR (400 MHz, $CDCl_3$) δ: 2.24 (m, 2H), 3.41 (t, 2H, *J* = 6.88 Hz), 4.15 (t, 2H, *J* = 5.95 Hz), 6.27 (d, 1H, *J* = 9.49 Hz), 6.81 (d, 1H, *J* = 2.37 Hz), 6.87 (dd, 1H, *J* = 2.47 and 8.59 Hz), 7.38 (d, 1H, *J* = 8.60 Hz), 7.64 (d, 1H, *J* = 9.49 Hz).

7-(4-bromobutoxy)-2H-chromen-2-one (1c). A white solid (yield 85%). ^{1}H NMR (400 MHz, $CDCl_3$) δ: 1.97-2.01 (m, 2H), 2.05-2.09 (m, 2H), 3.49 (t, 2H, *J* = 6.54 Hz), 4.05 (t, 2H, *J* = 6.04 Hz), 6.24 (d, 1H, *J* = 9.47 Hz), 6.79 (d, 1H, *J* = 2.34 Hz), 6.82 (dd, 1H, *J* = 2.38 and 8.54 Hz), 7.36 (d, 1H, *J* = 8.56 Hz), 7.63 (d, 1H, *J* = 9.44 Hz).

7-(5-bromopentyloxy)-2H-chromen-2-one (1d). A yellowish liquid (yield 89%). ^{1}H NMR (400 MHz, $CDCl_3$) δ: 1.61-1.66 (m, 2H), 1.82-1.86 (m, 2H), 1.92-1.95 (m, 2H), 3.43 (t, 2H, *J* = 6.69 Hz), 4.01 (t, 2H, *J* = 6.30 Hz), 6.22 (d, 1H, *J* = 9.46 Hz), 6.77 (d, 1H, *J* = 2.38 Hz), 6.81 (dd, 1H, *J* = 2.39 and 8.56 Hz), 7.35 (d, 1H, *J* = 8.59 Hz), 7.62 (d, 1H, *J* = 9.55 Hz).

7-(6-bromohexyloxy)-2H-chromen-2-one (1e). A white solid (yield 86%). ^{1}H NMR (400 MHz, $CDCl_3$) δ: 1.51-1.59 (m, 4H), 1.82-1.91 (m, 4H), 3.40 (t, 2H, *J* = 6.72 Hz), 4.01 (t, 2H, *J* = 6.35 Hz), 6.24 (d, 1H, *J* = 9.45 Hz), 6.78 (d, 1H, *J* = 2.40 Hz), 6.82 (dd, 1H, *J* = 2.42 and 8.54 Hz), 7.36 (d, 1H, *J* = 8.56 Hz), 7.62 (d, 1H, *J* = 9.46 Hz).

7-(7-bromoheptyloxy)-2H-chromen-2-one (1f). A white solid (yield 90%). ^{1}H NMR (400 MHz, $CDCl_3$) δ: 1.41-1.49 (m, 6H), 1.80-1.89 (m, 4H), 3.41 (t, 2H, *J* = 6.79 Hz), 4.00 (t, 2H, *J* = 6.45 Hz), 6.23 (d, 1H, *J* = 9.45 Hz), 6.79 (d, 1H, *J* = 2.35 Hz), 6.83 (dd, 1H, *J* = 2.31 and 8.55 Hz), 7.35 (d, 1H, *J* = 8.56 Hz), 7.63 (d, 1H, *J* = 9.44 Hz).

General procedures for synthesis of 7-(azidoalkyloxy)-2H-chromen-2-one (2a-2f).

7-Bromoalkyloxy-2H-chromen-2-one derivatives **(1a-f)** (3.72 mmol) and sodium azide (4.50 mmol) were added to 20 mL of water, and the mixture was irradiated at 150°C for 60 min using a microreactor (set to high absorption). The solvent was removed under reduced pressure, 30 mL DCM was added, and the mixture was washed with water (3 x 30 mL). The organic layer was then dried over sodium sulfate, and the solvent was removed under reduced pressure. The desired product was obtained after purification using flash column chromatography (DCM:Hexane = 3:1).

7-(2-azidoethoxy)-2H-chromen-2-one (2a). A yellow liquid (yield 60%). ^{1}H NMR (400 MHz, $CDCl_3$) δ: 3.65 (t, 2H, *J* = 4.86 Hz), 4.20 (t, 2H, *J* = 4.88 Hz), 6.27 (d, 1H, *J* = 9.49 Hz), 6.82 (s, 1H), 6.80 (d, 1H, *J* = 2.40 Hz), 7.32 (d, 1H, *J* = 8.59 Hz), 7.64 (d, 1H, *J* = 9.53 Hz).

7-(3-azidopropoxy)-2H-chromen-2-one (2b). A yellow liquid (yield 62%). ^{1}H NMR (400 MHz, $CDCl_3$) δ: 2.09 (tt, 2H, *J* = 6.23 and 6.22 Hz), 3.52 (t, 2H, *J* = 6.55 Hz), 4.10 (t, 2H, *J* = 5.92 Hz), 6.26 (d, 1H, *J* = 9.47 Hz), 6.83 (s, 1H), 6.85 (d, 1H, *J* = 2.41 Hz), 7.38 (d, 1H, *J* = 8.50 Hz), 7.64 (d, 1H, *J* = 9.49 Hz).

7-(4-azidobutoxy)-2H-chromen-2-one (2c). A yellow liquid (yield 65%). ^{1}H NMR (400 MHz, $CDCl_3$) δ: 1.74-1.84 (m, 2H), 1.87-1.94 (m, 2H), 1.87-1.94 (m, 2H), 3.37 (t, 2H, *J* = 6.71 Hz), 6.78 (s, 1H), 6.83 (d, 1H, *J* = 8.57 Hz), 7.36 (d, 1H, *J* = 8.57 Hz), 7.62 (d, 1H, *J* = 9.48 Hz).

7-(5-azidopentyloxy)-2H-chromen-2-one (2d). A yellow liquid (yield 70%). ^{1}H NMR (400 MHz, $CDCl_3$) δ: 1.56-1.63 (m, 2H), 1.69-1.73 (m, 2H), 1.78-1.89 (m, 2H), 3.32 (t, 2H, *J* = 6.62 Hz), 4.03 (t, 2H, *J* = 6.29 Hz), 6.25 (d, 1H, *J* = 9.47 Hz), 6.80 (s, 1H), 6.84 (d, 1H, *J* = 8.55 Hz), 7.36 (d, 1H, *J* = 8.55 Hz), 7.63 (d, 1H, *J* = 9.48 Hz).

7-(6-azidohexyloxy)-2H-chromen-2-one (2e). A yellow liquid (yield 65%). ^{1}H NMR (400 MHz, $CDCl_3$) δ: 1.43-1.54 (m, 4H), 1.61-1.68 (m, 2H), 1.80-1.86 (m, 2H), 3.29 (t, 2H, *J* = 6.83 Hz), 4.01 (t, 2H, *J* = 6.37 Hz), 6.24 (d, 1H, *J* = 9.48 Hz), 6.79 (s, 1H), 6.83 (d, 1H, *J* = 8.54 Hz), 7.36 (d, 1H, *J* = 8.55 Hz), 7.63 (d, 1H, *J* = 9.47 Hz).

7-(7-azidoheptyloxy)-2H-chromen-2-one (2f). A yellow liquid (yield 68%). ^{1}H NMR (400 MHz, $CDCl_3$) δ: 1.40-1.41 (m, 4H), 1.47-1.49 (m, 2H), 1.60-1.65 (m, 2H), 1.78-1.85 (m, 2H), 3.27 (t, 2H, *J* = 6.88 Hz), 4.02 (t, 2H, *J* = 6.43 Hz), 6.24 (d, 1H, *J* = 9.47 Hz), 6.82 (s, 1H), 6.84 (d, 1H, *J* = 2.33 Hz), 7.35 (d, 1H, *J* = 8.54 Hz), 7.63 (d, 1H, *J* = 9.47 Hz).

General procedures for synthesis of 7-(aminoalkoxy)-2H-chromen-2-one (3a-3f).

7-(azidoalkyloxy)-2H-chromen-2-one **(2a-f)** (4.32 mmol) and ammonium chloride (10.80 mmol) were added to ethanol/water (3:1) (20 mL), and zinc powder (6.48 mmol) was added to the mixture. The mixture was then irradiated at 150°C for 60 min using a microreactor (set to low absorption). The solvent was removed under reduced pressure. Ethyl acetate 40 mL and aqueous ammonia 2 mL were added, and the mixture was washed with brine, saturated sodium chloride, (3 x 40 mL). The ethyl acetate layer was dried over sodium sulfate, and the solvent was removed under reduced pressure. The desired product was obtained after purification with dissolve in acetone and HCl.

7-(2-aminoethoxy)-2H-chromen-2-one (3a). A white solid (yield 60%). ^{1}H NMR (400 MHz, $CDCl_3$) δ: 3.50 (t, 2H, *J* = 5.01 Hz), 4.38 (t, 2H, *J* = 4.99 Hz), 6.33 (d, 1H, *J* = 6.66 Hz), 6.99 (s, 1H), 7.04 (d, 1H, *J* = 2.35 Hz), 7.59 (d, 1H, *J* = 8.65 Hz), 7.95 (d, 1H, *J* = 9.42 Hz)

7-(3-aminopropoxy)-2H-chromen-2-one (3b). A white solid (yield 62%). ^{1}H NMR (400 MHz, $CDCl_3$) δ: 2.23 (tt, 2H, *J* = 6.80 and 6.07 Hz), 3.27 (t, 2H, *J* = 7.15 Hz), 4.29 (t, 2H, *J* = 5.72 Hz), 6.37 (d, 1H, *J* = 9.49 Hz), 7.03 (s, 1H), 7.05 (d, 1H, *J* = 2.39 Hz), 7.63 (d, 1H, *J* = 9.37 Hz), 8.00 (d, 1H, *J* = 9.48 Hz).

7-(4-aminobutoxy)-2H-chromen-2-one (3c). A white solid (yield 60%). ^{1}H NMR (400 MHz, $CDCl_3$) δ: 1.85-1.96 (m, 4H), 3.12 (t, 1H, *J* = 7.35 Hz), 4.15 (t, 2H, *J* = 5.65 Hz), 6.28 (d, 1H, *J* = 9.44 Hz), 6.87 (s, 1H), 6.95 (d, 1H, *J* = 8.68 Hz), 7.52 (d, 1H, *J* = 8.71 Hz), 7.91 (d, 1H, *J* = 9.45 Hz)

7-(5-aminopentyloxy)-2H-chromen-2-one (3d). A white solid (yield 64%). ^{1}H NMR (400 MHz, $CDCl_3$) δ: 1.54-1.60 (m, 2H), 1.72-1.78 (m, 2H), 1.83-1.87 (m, 2H), 3.05 (t, 2H, *J* = 7.56 Hz), 4.07 (m, 2H), 6.22 (d, 1H, *J* = 6.23 Hz), 6.75-6.77 (m, 1H), 6.86-6.88 (m, 1H), 7.43-7.46 (m, 1H), 7.84-7.86 (m, 1H).

7-(6-aminohexyloxy)-2H-chromen-2-one (3e). A white solid (yield 65%). ^{1}H NMR (400 MHz, $CDCl_3$) δ: 1.46-1.54 (m, 4H), 1.68-1.76 (m, 2H), 1.79-1.93 (m, 2H), 3.03 (t, 2H, *J* = 7.50 Hz), 4.08 (t, 2H, *J* = 6.50 Hz), 6.27 (d, 1H, *J* = 9.44 Hz), 6.82 (s, 1H), 6.90 (d, 1H, *J* = 8.69 Hz), 7.49 (d, 1H, *J* = 8.70 Hz), 7.89 (d, 1H, *J* = 9.45 Hz).

7-(7-aminoheptyloxy)-2H-chromen-2-one (3f). A white solid (yield 65%). ^{1}H NMR (400 MHz, $CDCl_3$) δ: 1.41-1.48 (m, 6H), 1.65-1.70 (m, 2H), 1.75-1.82 (m, 2H), 3.00 (t, 2H, *J* = 7.47 Hz), 4.05 (t, 2H, *J* = 6.47 Hz), 6.26 (d, 1H, *J* = 9.44 Hz), 6.79 (s, 1H), 6.88 (d, 1H, *J* = 8.71 Hz), 7.48 (d, 1H, *J* = 8.70 Hz), 7.87 (d, 1H, *J* = 9.44 Hz).

General procedures for synthesis of carbamate derivatives (4a-4f)

7-(Aminoalkoxy)-2H-chromen-2-one **(3a-3f)** (2.44 mmol) and triethylamine (3.65 mmol) were added to dichloromethane (20 ml) and the mixture was stirred at 0°C) for 5 min. Phenyl chloroformate (3.60 mmol) was added to the mixture and stirred at 0°C) for 30 min. The solvent was removed under reduced pressure. Ethyl acetate 50 mL was added, and the mixture was washed with sodium bicarbonate (3 x 100 mL), and the ethyl acetate layer was then dried over sodium sulfate. The solvent was removed under reduced pressure. The desired product was obtained after purification using flash column chromatography (10% EtOAc in DCM).

Phenyl (2-((2-oxo-2H-chromen-7-yl)oxy)ethyl)carbamate (4a). A white solid (yield 50%). mp = 162.1-162.8 °C; ^{1}H NMR (400 MHz, $CDCl_3$) δ: 3.71-3.75 (m, 2H), 4.18 (t, 2H, *J* = 5.05 Hz), 5.48 (s, 1H), 6.28 (d, 1H, *J* = 9.48 Hz), 6.84-6.89 (m, 2H), 7.13 (d, 2H, *J* = 7.72 Hz), 7.19-7.26 (m, 1H), 7.34-7.38 (m, 2H), 7.40 (d, 1H, *J* = 8.53 Hz), 7.65 (d, 1H, *J* = 9.49 Hz). HRMS (ESI-TOF) *m/z*: $[M+H]^+$ calcd for $C_{18}H_{16}NO_5$, 326.1028; found, 326.1028.

Phenyl (3-((2-oxo-2H-chromen-7-yl)oxy)propyl)carbamate (4b). A white solid (yield 52%). mp = 131.4-132.0°C; ^{1}H NMR (400 MHz, $CDCl_3$) δ: 2.13 (tt, 2H, J = 6.23 and 6.19 Hz), 3.15 (m, 2H), 4.14 (t, 2H, *J* = 5.83 Hz), 5.27 (s, 1H), 6.26 (d, 1H, *J* = 9.48 Hz), 6.82-6.89 (m, 2H), 7.12 (d, 2H, *J* = 7.95 Hz), 7.19 (t, 1H, *J* = 7.44 Hz), 7.33-7.39 (m, 3H), 7.64 (d, 1H, *J* = 9.48 Hz). HRMS (ESI-TOF) *m/z*: $[M+H]^+$ calcd for $C_{19}H_{18}NO_5$, 340.1185; found, 340.1185.

Phenyl (4-((2-oxo-2H-chromen-7-yl)oxy)butyl)carbamate (4c). A white solid (yield 60%). mp = 95.5-96.0°C; ^{1}H NMR (400 MHz, $CDCl_3$) δ: 1.76-1.83 (m, 2H), 1.88-1.95 (m, 2H), 3.35-3.40 (m, 2H), 4.07 (t, 2H, *J* = 6.00 Hz), 5.12 (s, 1H), 6.25 (d, 1H, *J* = 9.48 Hz), 6.81-6.85 (m, 2H), 7.12 (d, 2H, *J* = 7.69 Hz), 7.19 (t, 1H, *J* = 7.40 Hz), 7.34-7.38 (m, 3H), 7.63 (d, 1H, *J* = 9.48 Hz). HRMS (ESI-TOF) *m/z*: $[M+H]^+$ calcd for $C_{20}H_{20}NO_5$, 354.1341; found, 354.1339.

Phenyl (5-((2-oxo-2H-chromen-7-yl)oxy)pentyl)carbamate (4d). A white solid (yield 65%). mp = 99.2-99.8°C; ^{1}H NMR (400 MHz, $CDCl_3$) δ: 1.54-1.61 (m, 2H), 1.64-1.71 (m, 2H), 1.84-1.91 (m, 2H), 3.29-3.74 (m, 2H), 4.03 (t, 2H, *J* = 6.28 Hz), 5.06 (s, 1H), 6.24 (d, 1H, *J* = 9.47 Hz), 6.80-6.85 (m, 2H), 7.11-7.13 (m, 2H), 7.17-7.21 (m, 1H), 7.26-7.37 (m, 3H), 7.63 (d, 1H, *J* = 9.48 Hz). HRMS (ESI-TOF) *m/z*: $[M+H]^+$ calcd for $C_{21}H_{22}NO_5$, 368.1498; found, 368.1498.

Phenyl (6-((2-oxo-2H-chromen-7-yl)oxy)hexyl)carbamate (4e). A white solid (yield 62%). mp = 86.8-87.5°C; ^{1}H NMR (400 MHz, $CDCl_3$) δ: 1.45-1.52 (m, 2H), 1.54-1.55 (m, 2H), 1.59-1.66 (m, 2H), 1.81-1.87 (m, 2H), 3.27-3.32 (m, 2H), 4.02 (t, 2H, *J* = 6.37 Hz), 5.03 (s, 1H), 6.24 (d, 1H, *J* = 9.47 Hz), 6.80-6.84 (m, 2H), 7.12 (d, 2H, *J* = 7.89 Hz), 7.17-7.21 (m, 1H), 7.26-7.37 (m, 3H), 7.36 (d, 1H, *J* = 9.48 Hz). HRMS (ESI-TOF) *m/z*: $[M+H]^+$ calcd for $C_{22}H_{24}NO_5$, 382.1654; found, 382.1663.

Phenyl (7-((2-oxo-2H-chromen-7-yl)oxy)heptyl)carbamate (4f). A white solid (yield 60%). mp = 97.0-97.8°C; ^{1}H NMR (400 MHz, $CDCl_3$) δ: 1.41-1.43 (m, 4H), 1.46-1.54 (m, 2H), 1.57 (s, 1H), 1.58-1.62 (m, 2H), 1.79-1.84 (m, 2H), 3.25-3.40 (m, 2H), 4.01 (t, 2H, *J* = 6.46 Hz), 50.1 (s, 1H), 6.24 (d, 1H, *J* = 9.48 Hz), 6.80 (m, 2H), 7.11-7.13 (m, 2H), 7.18-7.20 (m, 1H), 7.34 (s, 1H), 7.36 (d, 2H, *J* = 8.47 Hz), 7.63 (d, 1H, *J* = 9.48 Hz). HRMS (ESI-TOF) *m/z*: $[M+H]^+$ calcd for $C_{23}H_{26}NO_5$, 396.1811; found, 396.1820.

Pharmacological evaluation

The inhibitory activities of all compounds against acetylcholinesterases (AChEs) were evaluated using the Ellman method (Ellman et al., 1961). In this method, ChE are obtained from an electric eel. The assay utilized 3.8 nM of acetylthiocholine chloride (ATCC) as a substrate for ChE. Upon enzymatic hydrolysis, ATCC was broken down to thiocholine and acetate. The resulting thiocholine subsequently reacted with 3 mM of 5,5′-dithiobis-(2-nitrobenzoic acid) (DTNB) to yield 2-nitrobenzoate-5-mercaptothiocholine and the yellow-colored 5-thio-2-nitrobenzoate (TNB) (Fig. 6). The rate of colour formation, directly proportional to ChE activity, was monitored using a UV-visible spectrophotometer. Under UV-visible radiation, TNB exhibited a characteristic absorption maximum (λmax) at 405 nm. Neostigmine was used as the positive control in this study.

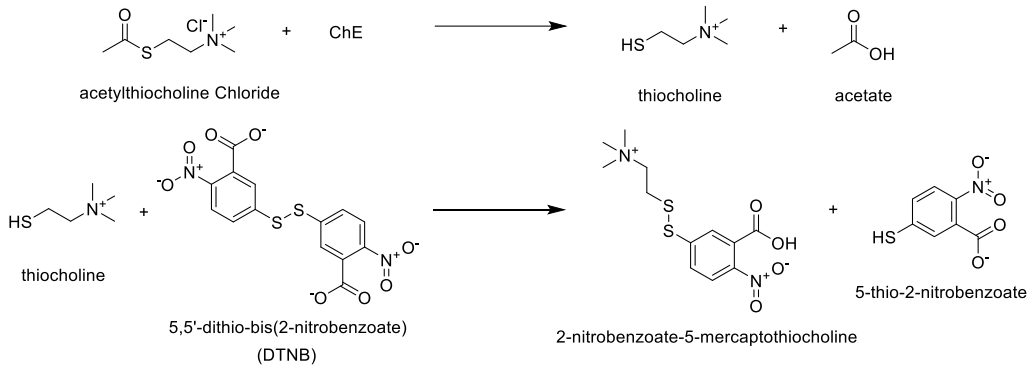

Figure 6 Ellman reaction between thiocholine and DTNB, where the thiocholine was obtained previously from the hydrolysis of acetylthiocholine chloride by ChE

Results and Discussion

In this study, we designed a novel series of carbamate derivatives to develop compounds capable of interacting with the PAS of acetylcholinesterase to inhibit β-amyloid aggregation through a pseudo-irreversible mechanism. We selected a coumarin nucleus as the core structure for PAS interaction and incorporated a carbamate group as the key functionality to facilitate carbamylation reaction with the catalytic serine residue. Specifically, 7-hydroxycoumarin was linked to a phenyl carbamate moiety via spacers of varying methylene chain lengths (2-7 carbon units) to yield compounds **4a- 4f**. In our preliminary investigation, we evaluated the acetylcholinesterase inhibitory activities of these synthesized compounds at 100 μM concentration using Ellman's colorimetric method.

As shown in Table 1, **4a and 4b**, containing 2- and 3-methylene unit spacers, respectively, exhibited minimal inhibitory activity (15.8% inhibition at 100 μM). Interestingly, progressive elongation of the spacer resulted in enhanced inhibitory potency. **4c-4e** demonstrated improved inhibitory activities with per cent inhibition values of 22.9%, 36.1%, and 63.7%, respectively. **4f**, featuring the longest spacer (7 methylene units), exhibited the highest *Electrophorus electricus* acetylcholinesterase (*Ee*AChE) inhibitory activity with 73.8% inhibition. However, when compared to the reference compound neostigmine (96.3% inhibition), none of our synthesized derivatives demonstrated superior inhibitory capacity against *Ee*AChE. These findings prompted us to hypothesize that our designed compounds contain carbamate functionalities with a weaker group-leaving properties. We postulated that extended compound-enzyme incubation periods during pharmacological evaluation might allow sufficient time for the carbamylation reaction between the carbamate functionality and the catalytic serine residue (Figure 7), potentially enhancing inhibitory activity. To test this hypothesis, compounds **4e** and **4f** were subjected to additional assays with increased incubation times (30 and 60 min compared to the standard 15 min). Contrary to our expectations, the results revealed that prolonged incubation times led to diminished inhibitory activities, with per cent inhibition values for both compounds decreasing to below 40% (Fig. 8). This observation contrasted with the behavior of the pseudo-irreversible inhibitor neostigmine, whose inhibitory activity remained unaffected by extended incubation periods. These results strongly suggest that our designed compounds do not inhibit acetylcholinesterase through a pseudo-irreversible mechanism as observed with neostigmine, indicating that the carbamate functionality fails to carbamylate the serine residue at CS of the enzyme.

Table 1 Percent inhibition of carbamate derivatives, RKNU026 and neostigmine against *Ee*AChE

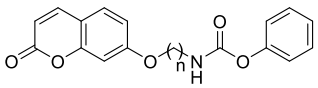

No.	n	% Inhibition[a]	No.	n	% Inhibition[a]
4a	2	15.8 ± 3.3	**4e**	6	63.7 ± 6.9
4b	3	15.8 ± 2.7	**4f**	7	73.8 ± 4.5
4c	4	22.9 ± 2.8	RKNU026	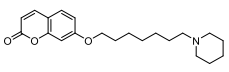	98.2 ± 0.4
4d	5	36.1 ± 4.5	Neostigmine	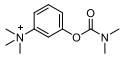	96.3 ± 0.2

[a]% inhibition of compounds was measured at a concentration of 100 μM using Ellman's method. The results are presented as mean ± standard error of the mean (SEM) of at least three independent experiments.

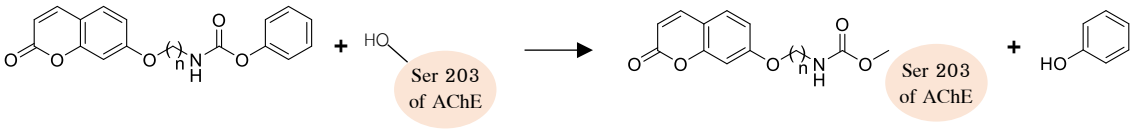

Figure 7 Proposed carbamylation reaction of 4a–4f with amino acid serine at CS of AChE

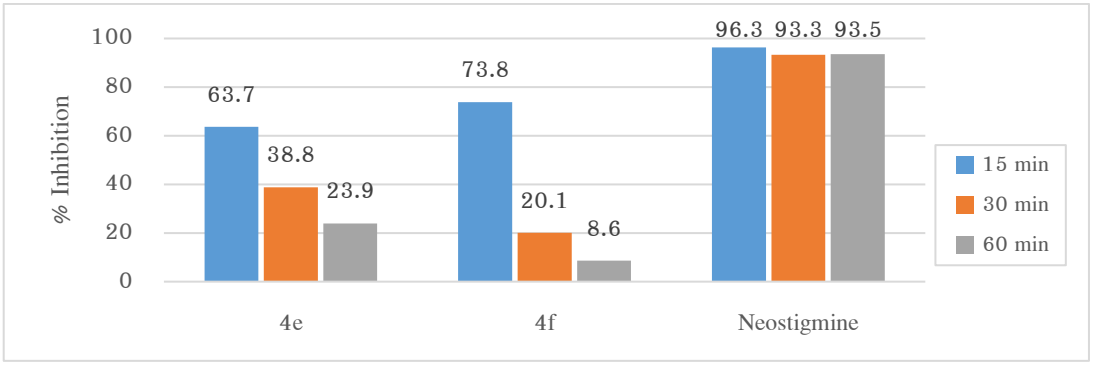

Figure 8 Graphical illustration showing the influence of incubation time on inhibitory activities against *Ee*AChE of RKNU153 (**4e**), RKNU154 (**4f**), and neostigmine measured at a concentration of 100 μM using Ellman's method

Structurally, **4f** resembles a previously identified AChE inhibitor RKNU026, with both compounds featuring a coumarin ring linked to a nitrogen atom via a 7-methylene unit spacer. However, **4f** additionally contains a carbamate functionality attached to the nitrogen atom. Comparative analysis revealed that this structural modification resulted in decreased *Ee*AChE inhibitory activity relative to RKNU026. This observation suggests that the basic nitrogen in RKNU026 plays a crucial role in facilitating cation-π interactions with residues in the MGS of the enzyme (Fig.9). Consequently, the reduced basicity of the nitrogen atom in **4f** contributes to its diminished inhibitory potency against *Ee*AChE. Additionally, steric hindrance introduced by the pendant benzyl group on the carbamate functionality may further contribute to the observed decrease in inhibitory activity.

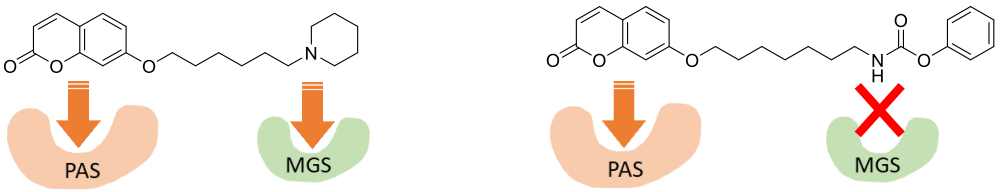

Figure 9 2D-Diagram illustrates binding interaction between RKNU026 (left) and 4f (right), and *Ee*AChE

Conclusion

In this study, we designed and synthesized a series of novel carbamate derivatives featuring a 7-hydroxycoumarin moiety linked to a carbamate functionality through spacers of varying methylene chain lengths (2–7 carbon units). At a concentration of 100 μM, both compounds **4e** and **4f** demonstrated the most potent *Ee*AChE inhibitory activity with 63.7% and 73.8% inhibition. Unlike the reference compound neostigmine, extended incubation periods during pharmacological evaluation led to diminished inhibitory

activities for **4e** and **4f**. These findings provide compelling evidence that our compounds do not interact with AChE through a pseudo-irreversible mechanism.

Our pharmacological evaluation revealed significant mechanistic differences between compounds **4e** and **4f** compared to neostigmine. While neostigmine effectively carbamylates the catalytic serine residue, compounds **4e** and **4f** do not engage in this critical covalent interaction. Additionally, unlike the previously reported RKNU026, compounds **4e** and **4f** lack the capacity to form cation-π interactions with residues in the middle gorge region, which accounts for their moderate inhibitory potency against AChE.

These structure-activity insights provide valuable direction for future optimization strategies to enhance both binding affinity and mechanistic interactions with AChE. The findings presented herein establish a foundation for the continued development of coumarin-based carbamate derivatives as potential AChE inhibitors with improved pharmacological profiles.

Acknowledgments

The authors gratefully acknowledge Dr. Nitra Nuengchamnong of the Faculty of Sciences, Naresuan University, for valuable technical assistance. Thanks also to Mr Roy I. Morien of the Naresuan University Graduate School for his editing of the grammar, syntax and general English expression in this manuscript.

Author Contributions

Pun Chirat, Thongchai Kanchanasuwan, and Wetchaporn Wetchakit: contributed equally in Chemical synthesis, Compound purification and identification, Computational modeling, In *vitro* testing.

Sutthatip Markmee: Data collection and analysis, Figure preparation, Manuscript writing.

Ruengwit Kitbunnadaj: Project conceptualization, Research supervision, Funding acquisition, Data analysis, Manuscript review and editing.

Conflict of Interests

All authors declare that they have no conflicts of interest.

Funding

There is no financial support for the research in this article.

References

Amin, K. M., Rahman, D. E. A., Allam, H. A., & El-Zoheiry, H. H. (2021). Design and synthesis of novel coumarin derivatives as potential acetylcholinesterase inhibitors for Alzheimer's disease. *Bioorganic Chemistry, 110*, 104792. https://doi.org/10.1016/j.bioorg.2021.104792

Bar-On, P., Millard, C. B., Harel, M., Dvir, H., Enz, A., Sussman, J. L., & Silman, I. (2002). Kinetic and structural studies on the interaction of cholinesterases with the anti-Alzheimer drug rivastigmine. *Biochemistry, 41*(11), 3555-3564. https://doi.org/10.1021/bi020016x

Bartolini, M., Cavrini, V., & Andrisano, V. (2007). Characterization of reversible and pseudo-irreversible acetylcholinesterase inhibitors by means of an immobilized enzyme reactor. *Journal of Chromatography A, 1144*(1), 102-110. https://doi.org/10.1016/j.chroma.2006.11.029

Bartus, R. T., Dean, R. L., Beer, B., & Lippa, A. S. (1982). The cholinergic hypothesis of geriatric memory dysfunction. *Science, 217*(4558), 408-414. https://doi.org/10.1126/science.7046051

Bennion, B. J., Lau, E. Y., Fattebert, J., Huang, P., Schwegler, E., Corning, W., & Lightstone, F. C. (2013). Modeling the binding of CWAs to AChE and BuChE. *Military Medical Science Letters, 82*(3), 102-114. https://doi.org/10.31482/mmsl.2013.015

Carvajal, F. J., & Inestrosa, N. C. (2011). Interactions of AChE with Abeta Aggregates in Alzheimer's Brain: Therapeutic Relevance of IDN 5706. *Frontiers in Molecular Neuroscience, 4*, 19. https://doi.org/10.3389/fnmol.2011.00019

Chaudhaery, S. S., Roy, K. K., Shakya, N., Saxena, G., Sammi, S. R., Nazir, A., Nath, C., & Saxena, A. K. (2010). Novel carbamates as orally active acetylcholinesterase inhibitors found to improve scopolamine-induced cognition impairment: pharmacophore-based virtual screening, synthesis, and pharmacology. *Journal of Medicinal Chemistry, 53*(17), 6490-6505. https://doi.org/10.1021/jm100573q

Chaudhary, R. K., Mateti, U. V., Khanal, P., Rawal, K. B., Jain, P., Patil, V. S., Shrivastava, A. K., & Patil, B. (2024). Alzheimer's Disease: Epidemiology, Neuropathology, and Neurochemistry. *In Computational and Experimental Studies in Alzheimer's Disease* (pp. 1-14). CRC Press.

Chen, H. M., Shen, K., Ji, L., McGrath, C., & Chen, H. (2025). Patterns and trends in the burden of Alzheimer's disease and related dementias in China (1990-2021) and predictions to 2040. *Journal of Alzheimer's Disease, 105*(3), 882-892. https://doi.org/10.1177/13872877251333108

Cohen, S. G., Chishti, S. B., Bell, D. A., Howard, S. I., Salih, E., & Cohen, J. B. (1991). General occurrence of binding to acetylcholinesterase-substrate complex in noncompetitive inhibition and in inhibition by substrate. *Biochimica et Biophysica Acta, 1076*(1), 112-122. https://doi.org/10.1016/0167-4838(91)90227-q

De Ferrari, G. V., Canales, M. A., Shin, I., Weiner, L. M., Silman, I., & Inestrosa, N. C. (2001). A structural motif of acetylcholinesterase that promotes amyloid beta-peptide fibril formation. *Biochemistry, 40*(35), 10447-10457. https://doi.org/10.1021/bi0101392

de Souza, G. A., da Silva, S. J., Del Cistia, C. d. N., Pitasse-Santos, P., Pires, L. d. O., Passos, Y. M., Cordeiro, Y., Cardoso, C. M., Castro, R. N., & Sant'Anna, C. M. R. (2019). Discovery of novel dual-active 3-(4-(dimethylamino) phenyl)-7-aminoalcoxy-coumarin as potent and selective acetylcholinesterase inhibitor and antioxidant. *Journal of Enzyme Inhibition and Medicinal Chemistry, 34*(1), 631-637. https://doi.org/10.1080/14756366.2019.1571270

De Vita, D., Pandolfi, F., Ornano, L., Feroci, M., Chiarotto, I., Sileno, I., Pepi, F., Costi, R., Di Santo, R., & Scipione, L. (2016). New N, N-dimethylcarbamate inhibitors of acetylcholinesterase: Design synthesis and biological evaluation. *Journal of Enzyme Inhibition and Medicinal Chemistry, 31*(sup4), 106-113. https://doi.org/10.1080/14756366.2016.1220377

Dvir, H., Silman, I., Harel, M., Rosenberry, T. L., & Sussman, J. L. (2010). Acetylcholinesterase: from 3D structure to function. *Chemico-Biological Interactions, 187*(1-3), 10-22. https://doi.org/10.1016/j.cbi.2010.01.042

Ellman, G. L., Courtney, K. D., Andres, V. J., & Feather-Stone, R. M. (1961). A new and rapid colorimetric determination of acetylcholinesterase activity. *Biochemical Pharmacology, 7*, 88-95. https://doi.org/10.1016/0006-2952(61)90145-9

Garcia-Ayllon, M. S., Small, D. H., Avila, J., & Saez-Valero, J. (2011). Revisiting the Role of Acetylcholinesterase in Alzheimer's Disease: Cross-Talk with P-tau and beta-Amyloid. *Frontiers in Molecular Neuroscience, 4*, 22. https://doi.org/10.3389/fnmol.2011.00022

Gupta, S., Fallarero, A., Jarvinen, P., Karlsson, D., Johnson, M. S., Vuorela, P. M., & Mohan, C. G. (2011). Discovery of dual binding site acetylcholinesterase inhibitors identified by pharmacophore modeling and sequential virtual screening techniques. *Bioorganic & Medicinal Chemistry Letters, 21*(4), 1105-1112. https://doi.org/10.1016/j.bmcl.2010.12.131

Hebert, L. E., Weuve, J., Scherr, P. A., & Evans, D. A. (2013). Alzheimer disease in the United States (2010-2050) estimated using the 2010 census. *Neurology, 80*(19), 1778-1783.

Hiranyaekaphap, T., Srimongkolpithak, N., Wongchang, T., Poowaruttanawiwat, P., Rattanamanee, K., & Kitbunnadaj, R. (2014). Discovery of novel cholinesterase inhibitor (RKNU026) with beta-amyloid aggregation inhibitory activity. *The Thai Journal of Pharmaceutical Sciences, 38*, 4-7. https://doi.org/10.56808/3027-7922.1992

Inestrosa, N. C., Alvarez, A., Dinamarca, M. C., Perez-Acle, T., & Colombres, M. (2005). Acetylcholinesterase-amyloid-beta-peptide interaction: effect of Congo Red and the role of the Wnt pathway. *Current Alzheimer Research, 2*(3), 301-306. https://doi.org/10.2174/1567205054367928

Inestrosa, N. C., Dinamarca, M. C., & Alvarez, A. (2008). Amyloid-cholinesterase interactions. Implications for Alzheimer's disease. The FEBS Journal, 275(4), 625-632. https://doi.org/10.1111/j.1742-4658.2007.06238.x

Kryger, G., Silman, I., & Sussman, J. L. (1999). Structure of acetylcholinesterase complexed with E2020 (Aricept): implications for the design of new anti-Alzheimer drugs. *Structure, 7*(3), 297-307. https://doi.org/10.1016/s0969-2126(99)80040-9

Lanctôt, K. L., Hahn-Pedersen, J. H., Eichinger, C., Freeman, C., Clark, A., Tarazona, L., & Cummings, J. (2024). Burden of illness in people with Alzheimer's disease: a systematic review of epidemiology, comorbidities and mortality. *The journal of prevention of Alzheimer's disease, 11*(1), 97-107. https://pmc.ncbi.nlm.nih.gov/articles/PMC10225771/

Liu, W., Deng, W., Gong, X., Ou, J., Yu, S., & Chen, S. (2025). Global burden of Alzheimer's disease and other dementias in adults aged 65 years and over, and health inequality related to SDI, 1990-2021: analysis of data from GBD 2021. *BMC Public Health, 25*(1), 1256. https://doi.org/10.1186/s12889-025-22378-z

Lomlim, L., & Nualnoi, T. (2011). New approach in development of acetylcholinesterase inhibitors for the treatment of Alzheimer's disease. *Thai Pharmaceutical and Health Science Journal, 6*(2), 157-173.

Morrison, A. S., & Lyketsos, c. (2005). The pathophysiology of Alzheimer's disease and directions in treatment. *Advanced Studies in Nursing*, *3*(8), 256-270.

Singbut, J., & Kaewket, S. (2010). Design and synthesis of novel coumarin derivatives as acetylcholinesterase inhibitors. Naresuan University.

Singh, Y. P., Kumar, N., Chauhan, B. S., & Garg, P. (2023). Carbamate as a potential anti-Alzheimer′s pharmacophore: A review. *Drug Development Research*, *84*(8), 1624-1651. https://doi.org/10.1002/ddr.22113

Song, M.-q., Min, W., Wang, J., Si, X.-X., Wang, X.-J., Liu, Y.-W., & Shi, D.-H. (2021). Design, synthesis and biological evaluation of new carbazole-coumarin hybrids as dual binding site inhibitors of acetylcholinesterase. *Journal of Molecular Structure*, *1229*, 129784.

Sun, Q., Peng, D.-Y., Yang, S.-G., Zhu, X.-L., Yang, W.-C., & Yang, G.-F. (2014). Syntheses of coumarin–tacrine hybrids as dual-site acetylcholinesterase inhibitors and their activity against butylcholinesterase, Aβ aggregation, and β-secretase. *Bioorganic & medicinal chemistry*, *22*(17), 4784-4791. https://doi.org/10.1016/j.bmc.2014.06.057

Yiannopoulou, K. G., & Papageorgiou, S. G. (2020). Current and future treatments in Alzheimer disease: an update. *Journal of central nervous system disease*, *12*, 1-12. https://doi.org/10.1177/1179573520907397

Zueva, I., Dias, J., Lushchekina, S., Semenov, V., Mukhamedyarov, M., Pashirova, T., Babaev, V., Nachon, F., Petrova, N., & Nurullin, L. (2019). New evidence for dual binding site inhibitors of acetylcholinesterase as improved drugs for treatment of Alzheimer′s disease. *Neuropharmacology*, *155*, 131-141.